

Spin-glass-like distribution of interaction fields in Pd-Ni alloys

T. D. Cheung* and J. S. Kouvel

Department of Physics, University of Illinois at Chicago, Chicago, Illinois 60680

(Received 6 June 1983)

Low-temperature heat-capacity measurements in various fixed magnetic fields were performed on several Pd-Ni alloys near the critical composition for ferromagnetism (~ 2.5 at. % Ni). From its variations with field H and temperature T , the specific-heat contribution from magnetic clusters (C_m) was separated from the local exchange enhancement, electronic, and lattice contributions. Simple model fits to $C_m(T, H)$ and to magnetization $M(H)$ data at low T show that the dilute concentrations of giant-moment clusters in these alloys have interaction (exchange and anisotropy) fields with a broad distribution in magnitude and direction. This spin-glass-like distribution of interaction fields, as it pertains to a weakly ferromagnetic alloy (2.8 at. % Ni), indicates a coexistence of ferromagnetic and spin-glass order. The $C_m(T, H)$ results for Pd-Ni are qualitatively very similar to those reported earlier for Ni-Cu near its critical composition for ferromagnetism.

INTRODUCTION

Disordered alloys of transition-metal impurities in a nonmagnetic host can be thought to raise two basic questions regarding their magnetism. The first is whether (and under what conditions) the impurity atoms form stable moments, and if stable-moment formation does occur, the second concerns the interactions among the randomly situated magnetic atoms and the ordered magnetic state(s) that they may produce. Both questions have received some interesting experimental answers in the case of Ni-Cu. Although in Cu (as in any other nonferromagnetic metal host) an isolated Ni atom does not have a stable local moment, neutron scattering¹ and magnetic²⁻⁴ measurements have shown that Ni atoms with highly Ni-rich local environments nucleate magnetic clusters having giant moments of $\sim 10\mu_B$. These experiments were performed on Ni-Cu alloys near the critical Ni concentration (~ 43 at. %) for ferromagnetism, whose onset was presumed to result from a percolation among the interacting clusters. Below this concentration, the clusters appeared to behave superparamagnetically, with little evidence of any intercluster coupling.⁴ However, more recent magnetic measurements have revealed a sharp low-temperature susceptibility cusp for a nearly ferromagnetic Ni-Cu alloy, which suggests the freezing in of a spin-glass state.⁵ Consistent with this finding, it was later deduced from the heat capacities of similar Ni-Cu alloys that the exchange fields on the magnetic clusters have a broad distribution in magnitude and direction.^{6,7} This spin-glass-like exchange-field distribution was seen to prevail even in a weakly ferromagnetic alloy, signifying perhaps the coexistence of different types of magnetic order.⁷

An alloy system of considerable related interest to us in Pd-Ni. In this case, the host being highly polarizable Pd, it has been found that isolated Ni atoms and Ni nearest-neighbor pairs make large locally enhanced contributions to the susceptibility and that critical local enhancement leading to the formation of giant-moment ($\sim 18\mu_B$) clusters occurs in groups of three or more Ni nearest neighbors.⁸⁻¹⁰ Moreover, our more recent measurements¹¹

have shown that as the Ni concentration in Pd approaches and exceeds the critical value (~ 2.5 at. %) for ferromagnetism, an increasing fraction of the Ni nearest-neighbor pairs also attain critical enhancement. Here also, each critically enhanced Ni-atom complex produces a large cluster moment ($\sim 12\mu_B$) which again includes the exchange-induced polarization of many neighboring Pd atoms, thus resembling the prototypal giant moment produced in Pd by a Co or Fe impurity atom.¹²

Regarding the nonferromagnetic Pd-Ni alloys of < 2.5 at. % Ni, our magnetic susceptibility measurements gave no obvious evidence of any coupling among the randomly situated magnetic clusters, which were seen to act basically as superparamagnets.¹¹ But some intercluster coupling in Pd-Ni must exist and, in view of the above-mentioned findings on Ni-Cu, its existence might very well be revealed and characterized by an appropriate calorimetric study. Hence we have carried out low-temperature heat-capacity measurements on several of the Pd-Ni alloys that we previously studied magnetically. Since the measurements were performed in various applied magnetic fields, the magnetic cluster contribution to the specific heat could be separated out fairly readily from the local-enhancement contribution as well as from the electronic and lattice heats. Our results are presented in this paper and compared to those of earlier heat-capacity measurements on Pd-Ni in zero field, which were interpreted without reference to magnetic clusters.¹³ The analysis of our calorimetric results for Pd-Ni, together with a more detailed analysis of our magnetization data for the same alloys, confirm the existence of dilute concentrations of giant-moment clusters and disclose that their interaction (exchange and anisotropy) fields have a broad spin-glass-like distribution, even in the case where the alloy is weakly ferromagnetic.

EXPERIMENTAL PROCEDURES

The Pd-Ni samples for our calorimetric work were three of the alloy buttons prepared earlier by arc-melting 99.995%-pure metals under argon, from each of which a

small piece had been cut for magnetic measurements.^{10,11} The buttons chosen, each weighing ~ 3 g, were those of 1.85, 2.35, and 2.8 at. % Ni, which represent both sides of the critical composition for ferromagnetism. They were annealed for 5 days at 1000°C and quenched into water, as had been done previously with the magnetometric samples.

The heat-capacity measurements were made between 1.2 and 15 K in magnetic fields up to 40 kOe. The adiabatic calorimeter employed has been described with regard to its previous use in the study of Ni-Cu.⁷ However, the acquisition and reduction of the calorimetric data have now been automated by means of a microprocessor-based controller, of which there is a detailed description in a recent instrumentation paper.¹⁴

RESULTS AND DISCUSSION

Our results for the temperature (T) dependence of the molar specific heat (C) of the three Pd-Ni samples in various fixed fields (H) are plotted as C/T vs T^2 in Fig. 1. The data obtained above ~ 11 K are omitted in order to avoid excessive compression of the low-temperature region, where nevertheless only about half of the measured points are plotted. This type of plot is normally intended for a data fit to a straight line expressed as

$$C/T = \gamma + \beta T^2, \quad (1)$$

where γ and β are taken to be the electronic and lattice heat coefficients, respectively. Such a straight-line

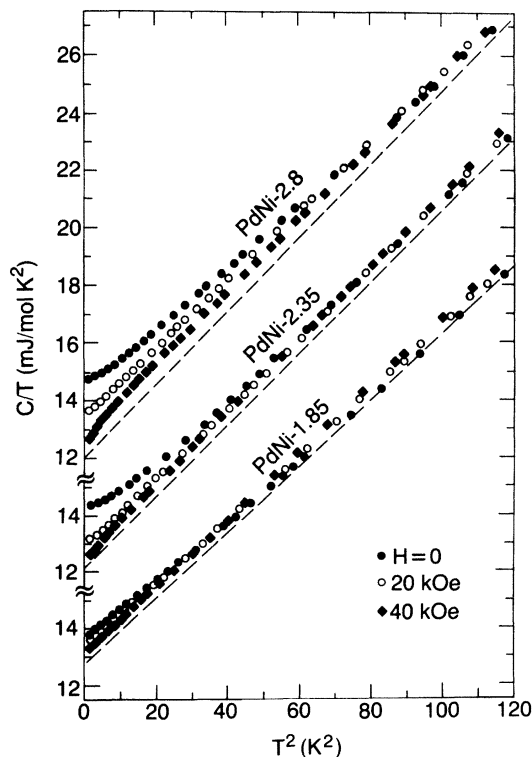


FIG. 1. C/T vs T^2 , where C is the total specific heat of Pd-Ni alloys (designated by at. % Ni) at temperature T in various magnetic fields. Data for different alloys are displaced vertically for clarity. Baselines shown dashed are discussed in the text.

behavior is clearly not followed by our zero-field results, which show a pronounced concave-upward curvature at low temperatures, especially for the alloys of 2.35 and 2.8 at. % Ni. However, as H is raised, the curvature in each case diminishes as C/T decreases towards values that lie on a linear extrapolation downward of the straight-line behavior of the zero-field results above ~ 10 K. If these linear extrapolations (represented in Fig. 1 by dashed lines) are regarded as baselines of reference, the experimental departures from them indicate an additional specific-heat contribution which is gradually suppressed at low T with increasing H and thus is presumably magnetic.

Leaving this magnetic specific-heat contribution for later discussion, let us consider the baselines themselves, which from Eq. (1) give the values of γ and β listed in Table I and plotted versus alloy composition in Fig. 2. Also plotted in this figure are the γ and β values deduced by Chouteau *et al.* from their heat-capacity data for various Pd-Ni compositions in zero field between 0.4 and 2 K.^{13,15} For a direct comparison with the latter, we show our analogous results for γ and β determined from linear fits to our zero-field C/T -vs- T^2 points below 3 K. The agreement is very close and supports the fact that the zero-field values for γ and β have a maximum and a minimum, respectively, as indicated by the dashed curves in Fig. 2. The deviations of these values from the γ and β of pure Pd were attributed by Chouteau *et al.*¹³ to a specific-heat contribution from the local exchange enhancement of the Ni solute atoms. However, the γ and β values that we determine from the baselines indicate in

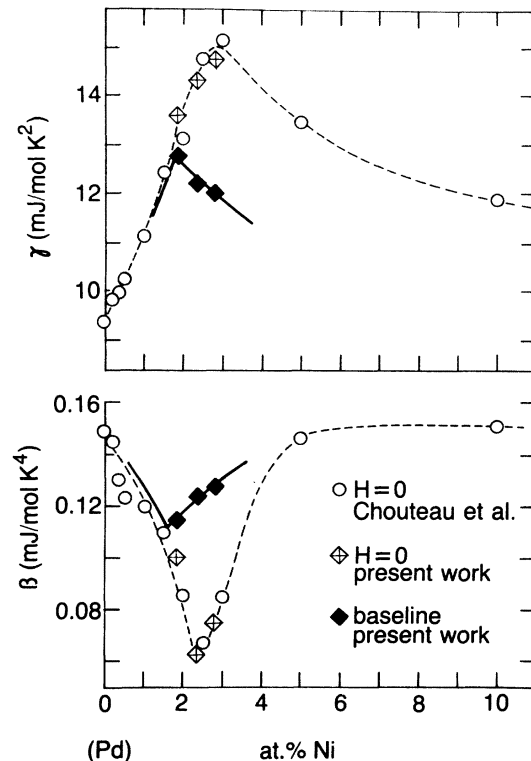


FIG. 2. Values of γ and β in Eq. (1) vs Pd-Ni alloy composition from zero-field data (Ref. 13 and present work) and from baselines (present work). Curves shown are guides to the eye.

Fig. 2 that the local-enhancement contribution is actually much smaller and peaks at a lower Ni concentration (1.8 at. %), which, as we have found earlier,¹¹ is approximately where the locally enhanced susceptibility is maximum.

Following Chouteau *et al.* but using our baseline values for γ and β , we will consider that the local-enhancement component of the specific heat of our Pd-Ni samples may be expressed as

$$C' = \gamma' T + \beta' T^3, \quad (2)$$

where $\gamma' = \gamma - \gamma_{\text{Pd}}$ and $\beta' = \beta - \beta_{\text{Pd}}$, and $\gamma_{\text{Pd}} = 9.40$ mJ/mol K² and $\beta_{\text{Pd}} = 0.149$ mJ/mol K⁴ are the electronic and lattice heat coefficients of pure Pd.¹³ The positive and negative values, respectively, for γ' and β' are listed in Table I. Plots of C' vs T based on these values are presented in Fig. 3 and are clearly very similar for all three alloys, exhibiting in each case a maximum C' at ~ 6 K. It should be noted that instead of the T^3 term in Eq. (2) a term of the form $T^3 \ln T$ is what is actually predicted from the local-enhancement model,¹⁶ but since these two forms are not distinguishable experimentally over our limited temperature range, the behavior of the curves in Fig. 3 may be considered to be representative. Another error in these curves could stem from our implicit assumption that C' does not change significantly with magnetic field and that the observed field dependence is predominantly that of the magnetic specific-heat component that lies above the fixed baselines (Fig. 1). But as will be described later, it is the latter component, when it is very small, whose determination may be seriously compromised by this assumption.

The magnetic component (C_m) of the specific heat, obtained for each alloy by subtracting the baseline from the total measured values of C , is plotted against temperature for various fixed fields in Fig. 4. Although the experimental error in the total specific heat is only about $\pm 0.5\%$, the baseline subtraction results in a much larger relative error in C_m , particularly at the higher temperatures. Nevertheless, it is clear in each case that C_m has a broad peak which shifts progressively to higher temperatures when the field is raised from zero to 20 kOe and then to 40 kOe. This behavior suggests that C_m depends in a Schottky-type fashion on the ratio T/H_T , where H_T is the total effective field consisting of the applied field plus the interaction (exchange and anisotropy) fields in the alloy. Indeed, the presence of the interaction fields is what presumably gives rise to the observed C_m at zero applied field. However, a simple Schottky function associated with a single discrete value of H_T behaves exponentially at low temperatures, whereas all our $C_m(T)$ results show a linear or nearly linear rise from the origin. An

TABLE I. Coefficients in Eqs. (1) and (2) for Pd-Ni alloys, as derived from the baselines in Fig. 1.

Ni content (at. %)	γ (mJ/mol K ²)	β (mJ/mol K ⁴)	γ' (mJ/mol K ²)	β' (mJ/mol K ⁴)
1.85	12.8	0.115	3.4	-0.034
2.35	12.2	0.124	2.8	-0.025
2.8	12.0	0.127	2.6	-0.022

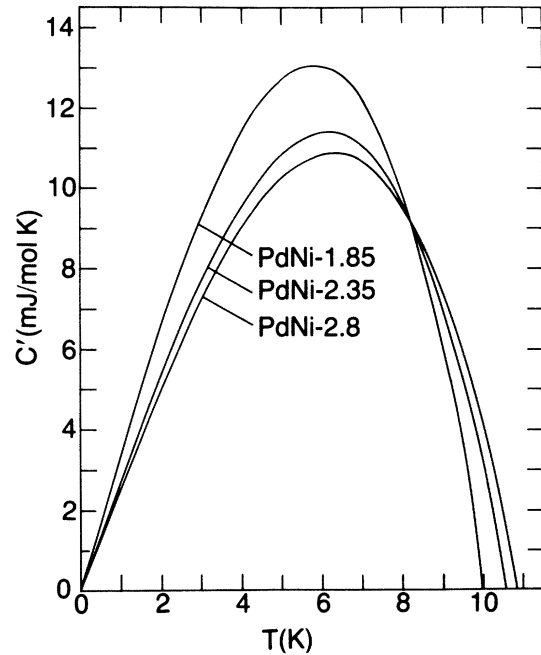


FIG. 3. Local-enhancement specific-heat component vs temperature for Pd-Ni alloys (designated by at. % Ni), as calculated from γ' and β' values listed in Table I.

essentially linear low-temperature variation of C_m was recently observed in Ni-Cu,^{6,7} and by analogy with similar variations seen in typical spin-glass alloys such as Cu-Mn,^{17,18} it was attributed to a broad exchange-field distribution $P(H_{\text{exch}})$ extending from positive to negative values of H_{exch} . This type of distribution in a spin-glass has been shown to derive from an oscillatory indirect-exchange Ruderman-Kittel-Kasuya-Yosida (RKKY) coupling among randomly situated local moments,^{19,20} which in Ni-Cu are the giant moments of magnetic clusters. Our $C_m(T)$ results in Fig. 4 appear to be reflecting a very similar situation in Pd-Ni.

In establishing the basic features of the interaction-field distribution in Pd-Ni, we will make use of not only the $C_m(T, H)$ results in Fig. 4 but also the low-temperature magnetization-versus-field behavior of the same alloys, which we reported earlier.¹¹ The M -vs- H data obtained at 2.4 K are shown in Fig. 5(a). Also shown by dashed lines are the high-field differential susceptibilities (χ') which were ascribed to the Pd host and to locally enhanced contributions from isolated Ni atoms and nearest-neighbor Ni pairs with subcritical environments.²¹ The quantity $M - \chi' H$, which is plotted against H in Fig. 5(b), was taken to represent the magnetization of the magnetic clusters nucleated by the spontaneously polarized Ni pairs and larger Ni-atom complexes.²¹ The high-field saturation values of $M - \chi' H$ and its initial slopes with H at various temperatures were the properties used in evaluating the average moments and concentrations of the magnetic clusters in the alloys. However, it should be noted that the curves in Fig. 5(b) differ in shape from a simple Brillouin-function curve which, if normalized to the experimental curves at low fields, would show a much faster approach to saturation than was observed. This

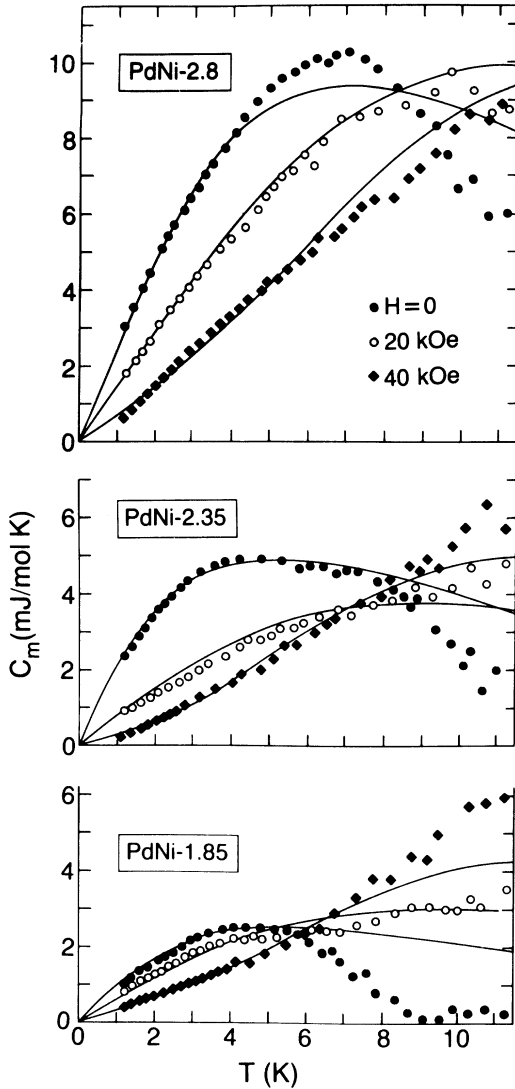


FIG. 4. Magnetic cluster specific-heat component vs temperature for Pd-Ni alloys (designated by at. % Ni) in various magnetic fields. Curves represent model fits described in the text.

discrepancy is similar to what was seen in Ni-Cu (Ref. 7) and suggests that the magnetic clusters in Pd-Ni may have an analogously wide spectrum of interaction fields.

To obtain simple-model fits to the magnetization curves in Fig. 5(b) and subsequently to the $C_m(T, H)$ results in Fig. 4, we consider each Pd-Ni alloy to have magnetic clusters of concentration c^* , average magnetic moment μ^* , and effective spin S . Furthermore, the clusters are assumed to have a total-field distribution $P(H_T)$ where, within an Ising model, H_T is the scalar sum of the net interaction field and the applied field H . The molar magnetization M at temperature T , normalized to its saturation value M_0 ($=N_A c^* \mu^*$, N_A being Avogadro's number) can then be expressed as

$$M/M_0 = \int_{x_{\min}}^{x_{\max}} B_S(\mu^* H_W x / kT) P(x) dx, \quad (3)$$

where $x = H_T/H_W$, H_W being the characteristic half-

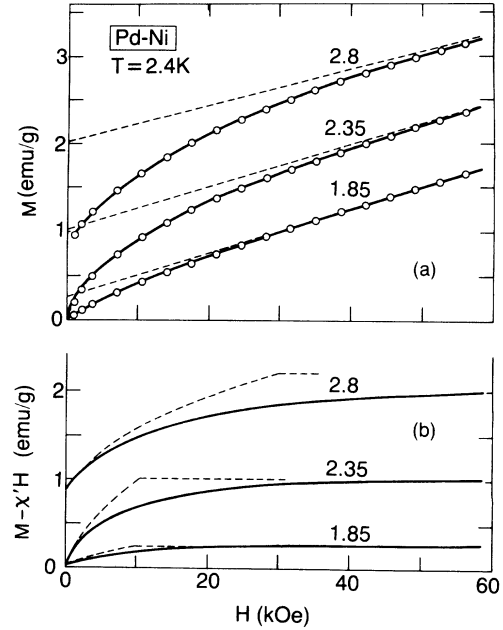


FIG. 5. (a) Magnetization (M) vs field (H) at 2.4 K for Pd-Ni alloys (in at. % Ni), as reported in Ref. 11; dashed lines signify high-field differential susceptibilities (χ'). (b) $M - \chi'H$ vs H derived from (a); dashed curves represent model fits for fixed H_W , as described in the text.

width of the distribution, and B_S is the Brillouin function for spin S . The integration limits define the range over which $P(x)$ is nonzero. Initially, $P(H_T)$ was considered to be rectangular in shape, as was done earlier in fitting the $C_m(T)$ data for Ni-Cu,^{6,7} in which case

$$P(x) = \frac{1}{2}, \quad x_{\max} = \bar{x} + 1, \quad x_{\min} = \bar{x} - 1, \quad (4)$$

where $\bar{x} = \bar{H}_T/H_W$, \bar{H}_T being the mean value of H_T located at the center of the symmetrical distribution. This simple distribution function is depicted in Fig. 6(a), and curves of M/M_0 vs \bar{H}_T/H_W calculated from Eqs. (3) and (4) for various values of $kT/\mu^* H_W$ are shown dashed in Fig. 6(b). In a nonferromagnetic case, where \bar{H}_T would essentially equal the applied field H , the curves represent normalized isotherms of M vs H , and we see that at very low T the curves rise almost linearly up to the saturation limit. Hence there is no possibility of achieving a reasonable fit to the low-temperature curves in Fig. 5(b) for the nonferromagnetic alloys of 1.85 and 2.35 at. % Ni, unless H_W is allowed to depend very strongly on H . To reduce the need for such an allowance, we shifted to a $P(H_T)$ function of Lorentzian form which, for calculational convenience, is truncated at $\bar{H}_T \pm 2H_W$, as depicted in Fig. 6(a). Equation (3) is then to be used in conjunction with

$$P(x) = \{2 \tan^{-1} 2[(x - \bar{x})^2 + 1]\}^{-1}, \quad (5)$$

$$x_{\max} = \bar{x} + 2, \quad x_{\min} = \bar{x} - 2,$$

where, as before, $\bar{x} = \bar{H}_T/H_W$. Curves of M/M_0 vs \bar{H}_T/H_W calculated on this basis are also shown in Fig. 6(b) where, as expected, they exhibit a more gradual approach to saturation at low temperatures.

In fitting the experimental magnetization curves in Fig.

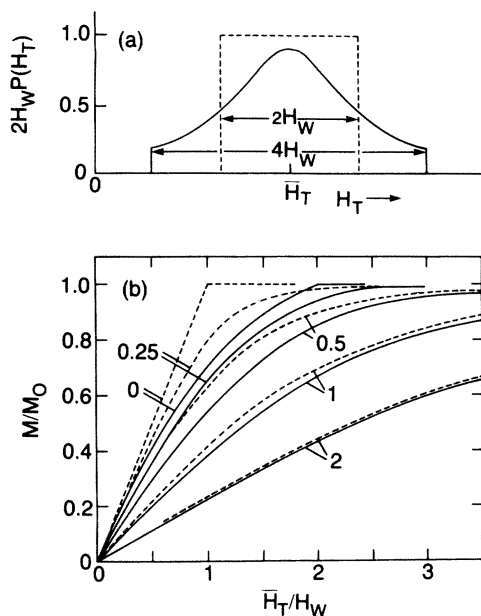


FIG. 6. (a) Truncated Lorentzian and rectangular distributions of total field (H_T) used in model analyses. (b) M/M_0 vs \bar{H}_T/H_W for various values of kT/μ^*H_W calculated for truncated Lorentzian and rectangular distributions (solid and dashed curves, respectively).

5(b) with curves derived from Eqs. (3) and (5), we assume from the results of our earlier analysis¹¹ that $S=2$ and that μ^* for the different alloys has the average values listed in Table II. Moreover, since $\bar{H}_T = H + \bar{H}_{\text{exch}}$, where \bar{H}_{exch} is the mean exchange field, we set $\bar{H}_{\text{exch}} = 0$ for the nonferromagnetic alloys and $\bar{H}_{\text{exch}} = 6$ kOe (with c^* chosen as described below) for the ferromagnetic alloy so that the calculated curves start at the origin and at the spontaneous magnetization value, respectively. For c^* and H_W , which govern the vertical and horizontal scaling of the calculated curves, values are chosen to give good fits to the experimental slopes and curvatures at $H=0$; these also are listed in Table II. The calculated curves are shown dashed in Fig. 5(b), and we see that they depart from the experimental curves at higher fields. This discrepancy can readily be removed by allowing H_W to in-

crease with increasing H . Indeed, for H_W raised gradually from its zero H values to the values listed in Table II for $H=50$ kOe, we obtain essentially perfect fits to the experimental curves.

For analogous cluster-model fits to the $C_m(T, H)$ results in Fig. 4, we make use of the expression

$$C_m = c^* N_A k \int_{x_{\min}}^{x_{\max}} C_S(\mu^* H_W x / 2kT) P(x) dx, \quad (6)$$

where $x = H_T/H_W$ as before, and the Schottky function for $S=2$,

$$C_S(y) = (y/2)^2 \text{csch}^2(y/2) - (5y/2)^2 \text{csch}^2(5y/2).$$

Again assuming a truncated Lorentzian form for $P(x)$, we combine Eq. (6) with Eq. (5) and generate curves of $C_m/c^* N_A k$ vs $2kT/\mu^* H_W$ for various values of \bar{H}_T/H_W . Typical examples in Fig. 7(a) serve to show that all the curves have a characteristic peak and that their emergence from the origin changes from linear to exponential with increasing \bar{H}_T/H_W , the curve for infinite \bar{H}_T/H_W corresponding to a simple Schottky function. Furthermore, as shown in Fig. 7(b), where the calculated curves are normalized at their peaks, the breadth of the curves about their peaks decreases with increasing \bar{H}_T/H_W .

In applying these curves to the $C_m(T, H)$ results in Fig. 4, we follow a procedure parallel to that described above for the magnetization curves. Thus we again set μ^* at the average values determined earlier¹¹ and adjust the vertical and horizontal scaling of the calculated $C_m(T)$ curves by means of c^* and H_W , respectively. We again also consider that $\bar{H}_T = H + \bar{H}_{\text{exch}}$, where \bar{H}_{exch} is zero except for the ferromagnetic 2.8-at. % Ni alloy for which it is an additional fitting parameter. Although the fits take into account the experimental peaks in $C_m(T)$, predominant weight is given to the more accurately determined behavior at the lowest temperatures. The curves of optimal fit thus obtained are shown in Fig. 4. They clearly follow the experimental $C_m(T)$ points quite closely at low temperatures, indicating a gradual change from a linear towards an exponential temperature dependence as the field on each alloy is increased. However, discrepancies set in at higher temperatures, especially in the 1.85-at. % Ni alloy case; other related problems with this case are

TABLE II. Cluster-model parameters for Pd-Ni alloys.

Ni content (at. %)	μ^* (μ_B)	From $M(H)$ at 2.4 K			From $C_m(T)$ at fixed H			
		\bar{H}_{exch} (kOe)	c^* (10^{-3})	$H_W(H)$ (kOe)	H (kOe)	\bar{H}_{exch} (kOe)	c^* (10^{-3})	H_W (kOe)
1.85	18	0	0.24	6(0)	0	0	0.57	17
				25(50)	20	0	0.71	20
					40	0	1.00	23
2.35	16	0	1.20	6(0)	0	0	1.17	18
				25(50)	20	0	0.89	20
					40	0	0.93	22
2.8	14	6	2.97	14(0)	0	15	2.01	23
				35(50)	20	15	2.04	28
					40	15	2.21	33

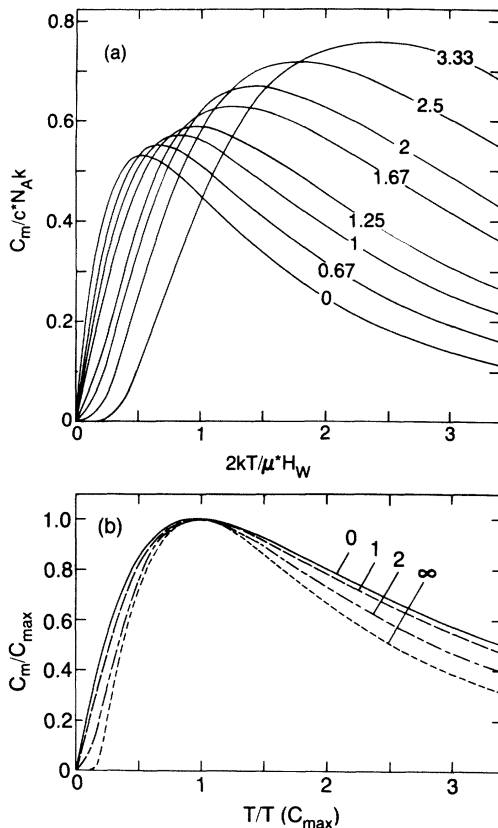


FIG. 7. (a) C_m/c^*N_Ak -vs- $2kT/\mu^*H_W$ curves for various values of \bar{H}_T/H_W calculated for truncated Lorentzian $P(H_T)$ distribution. (b) Some of the same curves shown normalized at their peaks; curve for infinite \bar{H}_T/H_W corresponds to simple Schottky function.

discussed below.

The parameter values used in calculating the $C_m(T)$ curves in Fig. 4 are listed in Table II for each alloy at each field of measurement (H). For the 2.35- and 2.8-at. % Ni alloys, the values for the cluster concentration (c^*) are reasonably the same for different H and are fairly consistent with the c^* values deduced from the magnetization curves. But for the 1.85-at. % Ni alloy, the c^* values derived from $C_m(T)$ vary considerably with H and are much larger than the value derived from $M(H)$. This unphysical situation may arise from the distinct possibility that the exchange-enhancement specific heat (C') at these temperatures (Fig. 3) has a field dependence similar to (though weaker than) that of C_m . Since the low-temperature positions of the baselines (which include C') were determined at high fields and were subsequently regarded as field independent, any such change in C' with H would appear as an increase in C_m (and hence in c^*), which would be relatively pronounced when the true C_m is small, as in the case of 1.85-at. % Ni. The values for the

exchange-field distribution halfwidth (H_W) for each alloy show a steady rise with increasing H , which is qualitatively in accord with theoretical prediction,²² and agree quite well with the H_W values derived from $M(H)$ at 50 kOe. However, the H_W values derived from $M(H)$ at zero fields are much smaller, which may stem from an intrinsic decrease of H_W with increasing temperature²³ since $M(H)$ was measured at 2.4 K, well above the temperature range emphasized in our model fitting of $C_m(T)$. An analogous rationale may account for the fact that the average exchange field (\bar{H}_{exch}) in the ferromagnetic 2.8-at. % Ni alloy is much smaller as derived from $M(H)$ at 2.4 K than the value derived from $C_m(T)$. The drop in \bar{H}_{exch} with increasing temperature, which this implies, is so large presumably because the ferromagnetic Curie point of this alloy is very low (~ 6 K).¹¹ Thus, if reasonable allowances are made for their field and temperature dependences, the parameter values deduced from our cluster-model analyses of the specific-heat and magnetization data for the three Pd-Ni alloys are fairly consistent.

In summary, our calorimetric and magnetic results show, after the contributions from local exchange enhancement have been separated away, that the dilute concentrations of giant-moment clusters in these Pd-Ni alloys have a broad distribution of exchange (and anisotropy) fields, both in magnitude and direction. This spin-glass-like exchange-field distribution in Pd-Ni presumably arises from indirect (RKKY) interactions among the randomly situated magnetic clusters and therefore resembles the situation produced by the frustrated demands of such interactions on individual magnetic atoms in a more typical spin-glass alloy.¹⁹ Moreover, with increasing at. % Ni in Pd, the cluster concentration rises and ultimately reaches a critical value for the onset of ferromagnetism, which probably results from a percolation among magnetic clusters that are overlapping. But even then, as our results for the weakly ferromagnetic 2.8-at. % Ni alloy testify, the exchange-field distribution remains quite broad, though displaced such that the average exchange field is no longer zero. This state of affairs, recently also found in weakly ferromagnetic Ni-Cu,⁷ appears to represent a coexistence of ferromagnetic and spin-glass order.²⁴ Such a coexistence in a random alloy can be expected to be spatially inhomogeneous, and this may well explain why recent neutron scattering studies of Pd-Ni indicate that the ferromagnetic correlation range does not diverge at the Curie temperature.²⁵

ACKNOWLEDGMENTS

We are grateful to Professor J. W. Garland and Mr. N. Kioussis for many helpful discussions of the theoretical context of this work, and to the National Science Foundation for support of this work under Grant No. DMR-81-11076.

*Present address: Department of Physics, Queens College, City University of New York, Flushing, NY 11367.

¹T. J. Hicks, B. Rainford, J. S. Kouvel, G. G. Low, and J. B. Comly, Phys. Rev. Lett. **22**, 531 (1969).

²C. G. Robbins, H. Claus, and P. A. Beck, Phys. Rev. Lett. **22**, 1307 (1969).

³J. P. Perrier, B. Tissier, and R. Tournier, Phys. Rev. Lett. **24**, 313 (1970).

- ⁴J. S. Kouvel and J. B. Comly, *Phys. Rev. Lett.* **24**, 598 (1970).
- ⁵D. W. Carnegie, C. J. Tranchita, and H. Claus, *J. Appl. Phys.* **50**, 7318 (1979).
- ⁶R. G. Aitken and J. S. Kouvel, *J. Magn. Magn. Mater.* **12**, 215 (1979).
- ⁷R. G. Aitken, T. D. Cheung, and J. S. Kouvel, *Phys. Rev. B* **24**, 1219 (1981).
- ⁸G. Chouteau, R. Tournier, and P. Mollard, *J. Phys. Colloq. (Paris)* **35**, C4-185 (1974).
- ⁹G. Chouteau, *Physica (Utrecht) B* **84**, 25 (1976).
- ¹⁰D. Sain and J. S. Kouvel, *Phys. Rev. B* **17**, 2257 (1978).
- ¹¹T. D. Cheung, J. S. Kouvel, and J. W. Garland, *Phys. Rev. B* **23**, 1245 (1981).
- ¹²Neutron scattering results for weakly ferromagnetic Pd-Ni reported by A. T. Aldred, B. D. Rainford, and M. W. Stringfellow [*Phys. Rev. Lett.* **24**, 897 (1970)] indicate magnetic clusters comparable in physical size to those in Pd-Co and Pd-Fe but with smaller moments than those deduced from subsequent magnetic measurements (Refs. 9–11), possibly due to cluster overlap effects.
- ¹³G. Chouteau, R. Fourneaux, R. Tournier, and P. Lederer, *Phys. Rev. Lett.* **21**, 1082 (1968).
- ¹⁴T. D. Cheung, W. K. Chan, and J. S. Kouvel, *Rev. Sci. Instrum.* **53**, 880 (1982).
- ¹⁵Zero-field calorimetric experiments performed on Pd-Ni by A. I. Schindler and C. A. Mackliet [*Phys. Rev. Lett.* **20**, 15 (1968)] gave results for γ very similar to those of Ref. 13, but results for β were not reported.
- ¹⁶P. Lederer and D. L. Mills, *Phys. Rev. Lett.* **19**, 1036 (1968); S. Doniach, S. Engelsberg, and W. F. Brinkman, *ibid.* **19**, 1040 (1968).
- ¹⁷L. T. Crane and J. E. Zimmerman, *J. Phys. Chem. Solids* **21**, 310 (1961).
- ¹⁸L. E. Wenger and P. H. Keesom, *Phys. Rev. B* **13**, 4053 (1976).
- ¹⁹W. Marshall, *Phys. Rev.* **118**, 1519 (1960); M. W. Klein and R. Brout, *ibid.* **132**, 2412 (1963).
- ²⁰As shown by L. R. Walker and R. E. Walstedt [*Phys. Rev. Lett.* **38**, 514 (1977)], $P(H_{\text{exch}})$ for a spin-glass vanishes near zero H_{exch} , but this effect on the specific heat would be observable only at temperatures well below those of the present measurements on Pd-Ni.
- ²¹Local-environment conditions for magnetic cluster formation in Pd-Ni have been studied theoretically by N. Kioussis and J. W. Garland [*Bull. Am. Phys. Soc.* **27**, 183 (1982)], whose results are basically in accord with the conditions deduced experimentally (Ref. 11).
- ²²M. W. Klein, *Phys. Rev.* **188**, 933 (1969).
- ²³M. W. Klein, *Phys. Rev.* **173**, 552 (1968).
- ²⁴Ferromagnetic and spin-glass states (and possible transitions between them) that can derive from an exchange-field distribution whose width is comparable to the average field have been discussed theoretically by S. Kirkpatrick and D. Sherrington [*Phys. Rev. B* **17**, 4384 (1978)].
- ²⁵S. K. Burke, R. Cywinski, E. J. Lindley, and B. D. Rainford, *J. Appl. Phys.* **53**, 8079 (1982).